

Interfacial Thickness in Bilayers of Poly(phenylene oxide) and Styrenic Copolymers

G. D. MERFELD,¹ A. KARIM,² B. MAJUMDAR,³ S. K. SATIJA,⁴ D. R. PAUL¹

¹ The University of Texas at Austin, Center for Polymer Research, Austin, Texas 78712

² Polymers Division, NIST, Gaithersburg, Maryland 20899

³ General Electric Plastics, Selkirk, New York 12158

⁴ Reactor Division, NIST, Gaithersburg, Maryland 20899

Received 24 April 1998; revised 26 June 1998; accepted 1 July 1998

ABSTRACT: Estimates for the thickness of the interface between poly (2,6-dimethyl-1,4-phenylene oxide) (PPO) and copolymers of styrene–acrylonitrile (SAN) and styrene–maleic anhydride (SMA) based on the theory of Helfand and Tagami are compared to neutron reflectivity (NR) measurements. Good agreement is found between the NR measurements and theoretical predictions that make use of a mean field binary interaction model and previously reported binary interaction energies. The techniques outlined in this work may be used to understand relationships between the mechanical properties of multiphase polymer blends and the fundamental thermodynamics of polymer interactions. © 1998 John Wiley & Sons, Inc. *J Polym Sci B: Polym Phys* 36: 3115–3125, 1998

Keywords: interfacial thickness; PPO; SAN; SMA; neutron reflectivity NR; binary interaction energies

INTRODUCTION

The properties of a multiphase polymer blend are determined in part by the nature of the polymer–polymer interface. The interfacial tension, γ , influences morphology development during melt mixing while interfacial thickness, λ , is related to the adhesion between the phases in the solid blend. A quantitative relation between the thermodynamic interaction energy and these interfacial properties was first proposed in the theory of Helfand and Tagami, and has since been correlated with experimental measurements with varying degrees of success. The goal of this study is to further investigate whether theory and experiment can be unified for polymer pairs of some technological importance.

To this end, a set of carefully designed neutron reflection experiments were performed to measure the interfacial thickness between poly (2,6-dimethyl-1,4-phenylene oxide) (PPO) and styrene–acrylonitrile (SAN) copolymers, and between PPO and styrene–maleic anhydride (SMA) copolymers. PPO and polystyrene (PS) are completely miscible; however, by incorporating increasing amounts of AN or MA repeat units into a copolymer with styrene, unfavorable interaction energies result, giving rise to immiscibility, with PPO creating an interface that varies in thickness as a function of the copolymer composition. For these blend systems, the overall interaction energy can be calculated using a mean-field binary interaction model expressed in terms of the interactions between repeat unit pairs. All the binary interaction energies needed for this study have been reported previously or can be extracted directly from reports of blend phase behavior. Pre-

Correspondence to: D. R. Paul

Journal of Polymer Science: Part B: Polymer Physics, Vol. 36, 3115–3125 (1998)
© 1998 John Wiley & Sons, Inc. CCC 0887-6266/98/173115-11

dictions of λ as a function of copolymer composition can be made by combining the binary interaction model with the Helfand–Tagami theory.

BACKGROUND

Many studies have reported measurements of interfacial properties using a variety of techniques. These include, for example, neutron and X-ray reflectometry, ellipsometry, and transmission electron microscopy to estimate interfacial thickness, and capillary thread breakup, pendant drop curvature, and imbedded-fiber retraction to estimate interfacial tension. A portion of this research has focused on block copolymers,^{1,2} while other studies have looked at the interface between two homopolymers, and to a lesser extent between a homopolymer and a random copolymer. Typically, a parameter such as temperature, molecular weight, or copolymer composition is varied in these studies.

The present study is motivated by the excellent agreement found between the measured interfacial thickness for bisphenol A polycarbonate (PC) and SAN for a single composition of 25 wt % AN and that calculated using the Helfand–Tagami theory. Mansfield³ reports a λ of 45 Å from neutron reflectivity measurements. Figure 1(a) shows λ , calculated in the limit of infinite molecular weight, as a function of SAN composition, and predicts a value of approximately 46 Å for the 25 wt % AN. The calculation is based on established binary interaction energy values⁴ of $B_{S/PC} = 0.43$, $B_{S/AN} = 6.8$, and $B_{PC/AN} = 4.5$ cal/cm³, and uses the unperturbed molecular dimensions for PC and SAN25 reported in Table I. Figure 1(b) compares calculations of the PC/SAN interfacial tension to values obtained by capillary thread instability measurements. Reasonable agreement is demonstrated, particularly with respect to the minimum in the composition dependence. The discrepancy is greatest at large AN compositions where it is suspected that higher viscosities cause capillary measurements to become increasingly difficult.

The system of polystyrene/poly (methyl methacrylate) (PMMA) has been studied extensively. Fernandez et al.^{6,7} and Anastasiadis et al.⁸ used neutron reflectivity to measure an interfacial thickness of 50 ± 10 Å. With estimates for the PS/PMMA binary interaction energy that range in value from 0.19 to 0.26 cal/cm³, the Helfand–Tagami theory predicts the interface to be approximately 35 to 45 Å thick. These calculations ac-

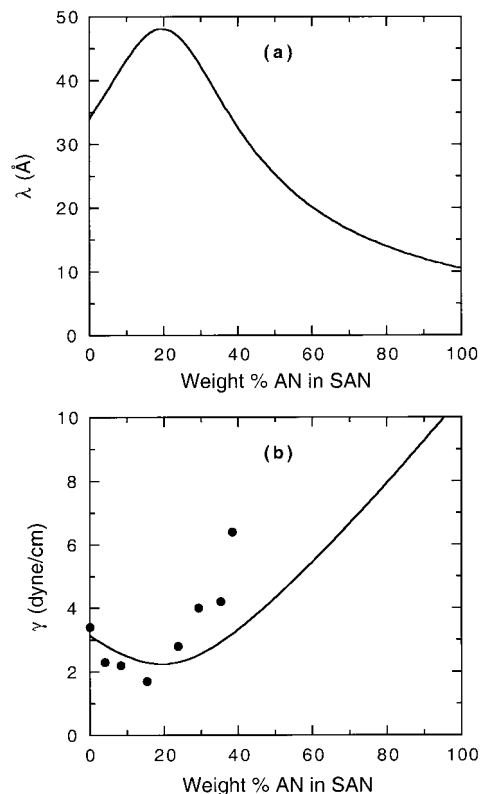


Figure 1. Interfacial properties of PC and SAN as a function of copolymer composition. (a) Interfacial thickness calculated assuming infinite molecular weight and using binary interaction energies reported in the text. (b) Interfacial tension calculations compared with measurements by capillary thread instability (see ref. 5).

count for the molecular weight of each polymer and use the unperturbed molecular dimensions for PS and PMMA given in Table I. The upper end of the predicted range is reasonably consistent with the experimental values. Furthermore, two independent studies^{13,14} report the PS/PMMA interfacial tension to be 1.2 ± 0.1 dyne/cm, which is within the range of 1.0 to 1.8 dyne/cm estimated by theory.

The agreement between experiment and theory has not been quite so favorable in other studies, however, and various efforts have been made to remedy or explain apparent discrepancies. Schubert and Stamm¹⁵ used NR to study PS/PMMA interfaces and found thicknesses ranging from 42 to 66 Å, depending on the PMMA molecular weight; they attempted to bring these values in line with their calculations by subtracting the as-prepared interfacial roughness. As pointed out by others, however, this correction is unfounded because the equilibrium of the annealed interface

Table I. Polymer Physical Properties

Polymer	M_w (g/mol) ^a	M_n (g/mol) ^a	Density (g/cm ³)	$(\langle r_0^2 \rangle / M)^{1/2}$ $\times 10^4$ (nm) ^b	$(b/v) \times 10^{-6}$ (Å ⁻²)
PS	—	—	—	650	—
PMMA	—	—	—	600	—
PC	—	—	—	920	—
dPPO	27,300	14,200	1.133	840	4.46
SAN15	182,000	83,000	1.064	725	1.59
SAN20	179,000	84,300	—	750	1.65
SAN25	152,000	77,000	1.078	775	1.69
SAN30	168,000	81,000	—	805	1.73
SAN40	122,000	61,000	1.092	850	1.79
SMA8	200,000	100,000	1.079	665	1.53
SMA14	178,000	92,000	1.104	675	1.62
SMA33	260,000	130,000	1.191	705	1.96

^a According to IFO 31-8, the term “molecular weight” has been replaced with the relative molecular mass, M_r . However, the conventional notation M_w and M_n (representing weight-average and number-average molecular weight) are used here.

^b SAN and SMA molecular dimensions calculated as linear function of copolymer composition using reported values of 650 nm for PS, 770 nm for SAN with 24 wt % AN, and 732 nm for SMA with 48 wt % MA.

should be independent of the initial state. More recently, work by Sferrazza et al.¹⁶ suggested that capillary waves in thin films may be a possible source of disagreement. The authors propose that thermally induced capillary waves can stabilize less diffuse interfaces in thin-film samples. This effect was documented in NR characterization of the interface between bilayers of PMMA (4000 to 9000 Å thick) and PS of varying thickness (50 to 20,000 Å). The interfacial thickness was shown to increase logarithmically as the PS top layer thickness increased to approximately 1000 Å, but then leveled off and became invariant for thicker samples. In the regime where these effects became negligible, the authors reported an interfacial thickness of 51 ± 7 Å, which is consistent with other reports.

A study of several homopolymer/copolymer systems using ellipsometry suggests that the predictive capability of the Helfand–Tagami theory may exclude highly diffuse interfaces.^{17–19} For immiscible blends of PMMA with SAN copolymers, theoretical predictions described the change in interfacial thickness as a function of copolymer composition; however, a large discrepancy existed in the magnitude of the measured and predicted values. Similar deviations were observed for immiscible blends of PS with S/MMA copolymers. The authors suggest that these interfaces, on the order of 100 Å thick, may be too broad to be accurately modeled by the Helfand and Tagami theory. They point out that the Helfand theory is

derived in the limit of strong segregation where interpenetration must be much smaller than the dimensions of the polymer coils. They note improved agreement for the system of PMMA with S/MMA copolymers where the interfaces are 100 Å or less in thickness, but large uncertainty in the ellipsometry measurements prevented critical comparison with theory.

INTERFACIAL THEORY

Helfand and Tagami first proposed a theory to predict the interfacial properties of immiscible, noncompressible polymers that balances energetics and conformational entropy at the interface. Later refinements by Helfand and Sapse²⁰ generalized the results to account for the properties of each polymer so that in the limit of infinite molecular weights the interfacial thickness is given by²¹

$$\lambda_\infty = \sqrt{\frac{2RT}{B}} (\beta_A^2 + \beta_B^2)^{1/2} \quad (1)$$

In this expression, B is the interaction energy density for the polymer pair and β_i is related to the dimension of the polymer coil as shown

$$\beta_i = \sqrt{\frac{\rho_i}{6}} (\langle r_i^2 \rangle / M_i)^{1/2} \quad (2)$$

where $\langle r_i^2 \rangle$ is the mean square unperturbed end-to-end chain distance and M_i is the molecular weight. Likewise, interfacial tension is expressed in the same nomenclature as

$$\gamma_\infty = \sqrt{\frac{RTB}{2}} (\beta_A + \beta_B) \left[1 + \frac{1}{3} \frac{(\beta_A - \beta_B)^2}{(\beta_A + \beta_B)^2} \right] \quad (3)$$

The interaction energy B used in eqs. (1) and (3) is the same as that in the classical Flory–Huggins theory

$$\Delta g_{\text{mix}} = RT \left[\frac{\rho_A \phi_A \ln \phi_A}{M_A} + \frac{\rho_B \phi_B \ln \phi_B}{M_B} \right] + B \phi_A \phi_B \quad (4)$$

It is convenient to use the interaction energy density in this formulation rather than the conventional dimensionless χ parameter because this avoids the awkward use of reference volumes, especially when the components of the overall interaction energy for copolymer systems are derived from multiple sources.

For a homopolymer/homopolymer system, such as PS/PMMA, B is simply the binary interaction energy density between the two repeat unit types. For the homopolymer/copolymer system of PPO/SAN (or analogously for PPO/SMA), an overall B can be calculated using the appropriate form of the binary interaction model, given here as

$$B = B_{\text{PPO/S}} \phi_S + B_{\text{PPO/AN}} \phi_{\text{AN}} - B_{\text{S/AN}} \phi_S \phi_{\text{AN}} \quad (5)$$

where ϕ_S and ϕ_{AN} are volume fractions of styrene and acrylonitrile in the SAN copolymer.

More recently, the Helfand–Tagami theory was extended by Broseta et al.²² to treat finite molecular weights by using an asymptotic approximation to square gradient theory. For the smallest molecular weights used in this study, the approximation leads to an underestimate of less than 5% relative to the full square gradient theory. The entropic gain associated with finite molecular weights gives rise to broadened interfaces and reduced interfacial tension with a correction to λ_∞ as shown

$$\lambda = \lambda_\infty \left[1 - \frac{2RT \ln 2}{B} \left(\frac{\rho_A}{M_A} + \frac{\rho_B}{M_B} \right) \right]^{-1/2}$$

This correction can increase λ on the order of 10–30%. Furthermore, it was demonstrated for the case of polydisperse systems that there is an

entropic advantage when small chains segregate to the interface. Small chains can lower the interfacial tension and increase the interfacial thickness.

EXPERIMENTAL

The physical properties of the polymers used in this study are listed in Table I. More detailed characterizations of the SAN and SMA copolymers have been reported previously.^{4,12,24} The perdeuterated PPO was provided by the General Electric Co.²⁵ The molecular dimensions used in the λ calculations, taken from the literature, are included in Table I as values of $(\langle r_o^2 \rangle / M)^{1/2}$, where $\langle r_o^2 \rangle$ is the unperturbed mean-square end-to-end distance.^{26–31} Typically, these values were estimated from viscometry or light-scattering measurements made in good solvents and then extrapolated to dimensions corresponding to theta conditions using the techniques of Stockmayer–Fixman or Kurata–Stockmayer. Dimensions for SAN and SMA were calculated as a linear function of copolymer composition based on values reported for PS, for a SAN containing 24 wt % AN, and for a SMA containing 48 wt % MA.

Bilayer samples of dPPO and SAN were prepared by first spin coating dPPO layers (~ 400 Å thick) from a solution containing 1.5 wt % polymer in toluene onto polished silicon wafers 10 cm in diameter and 5 mm thick. Next, SAN films (nominally 1200 Å thick) were spin cast from a solution of 3 wt % polymer in methyl ethyl ketone onto glass plates. Each SAN layer was floated off its glass plate onto a pool of water and then the dPPO-coated silicon wafer was used to pick up the floating SAN film; thus, a bilayer sample with the construction Si/dPPO/SAN was created. Samples were held under vacuum at room temperature for several hours to remove residual water or solvent. At least three annealing treatments were performed on each sample, the first at 140°C for 1.5 h, the second at 140°C for 9 h, and the third at 180°C for 0.5 h.

Difficulties with floating the SMA films made it necessary to reverse the construction order so that films of the SMA copolymers (~ 900 Å thick) were cast directly onto the silicon wafer, and dPPO films (~ 600 Å thick) were floated on top. Even with the reversed construction, however, it was difficult to produce high-quality samples owing in part to the brittleness of the dPPO films. Only three Si/SMA/dPPO bilayer samples were

Table II. Binary Interaction Energies

Interaction Pair	Reported Interaction Energy (cal/cm ³) (at T°C)	B _{ij} at 140°C (cal/cm ³) ^{a,f}	Polymer System	Method ^b	Reference
S/AN	B = 6.7 (25)	6.5	PMMA/SAN	A	32
	B = 6.8 (170)	6.9	SMA/SAN	A	12
	B = 7.0 (120)	7.0	PMMA/SAN	B	33
	B = 7.3 (30)	7.0	TMPC/SAN	B	11
PPO/S	χ = 0.121 - 77.9/T	-0.52 ^c	PPO/PS	C	34
	B = <-0.37 (180)	<-0.38	PPO/SMA	A	12
	χ = -0.043 (200)	-0.38	PPO/chlorinated styrenics	A	35, 36
	χ = 0.145 - 78/T	-0.34 ^c	PPO/PS	D	37
PPO/AN	—	9.7 - 11.3 ^d	PPO/SAN	A	38
S/MA	B = 10.6 (180)	10.8	PS/SMA	E	39
	B = 10.7 (170)	10.8	SMA/SAN	A	12
PPO/MA	B = 14.2 - 15.1 (180)	13.4 - 16.6 ^e	PPO/SMA	A	12

^a Calculated based on an equation of state correction except where noted otherwise.

^b A = Analysis of miscibility boundaries, B = analysis of LCST-type phase behavior, C = small angle neutron scattering, D = forward recoil spectrometry, E = critical molecular weight method.

^c χ calculated at 140°C then converted to B_{ij}.

^d Calculated using B_{PPO/S} = -0.52 or -0.34 and the report of phase separation at 140°C for a blend of PPO with SAN containing 11.5 wt % AN.

^e Recalculated from reported miscibility limits of PPO with SMA containing between 10–12 wt % MA and interactions summarized here.

^f To convert to S.I. units of J/cm³, multiply cal/cm³ by 4.187.

made and tested because of these limitations. These samples were annealed at temperatures of 140, 150, and 180°C for 3 to 8 h.

Neutron reflectivity experiments were performed on the NG7 reflectometer at the National Institute of Standards and Technology cold neutron research facility in Gaithersburg, MD. All samples were tested as cast and following each annealing treatment, in most cases with the incident neutron beam entering through the silicon substrate. A single layer of each polymer was also tested to directly measure the coherent scattering length density (b/v). These values were used to reduce the number of unknowns in fitting a reflectivity model to NR data. Table I records these fitted values, which are in good agreement with calculated estimates.

BINARY INTERACTION ENERGIES FOR PPO/SAN AND PPO/SMA

Binary interaction energies, B_{ij}, relevant to the polymers investigated have been evaluated previously. Table II summarizes the most refined estimates of these values that are available to date (to convert to S.I. units of J/cm³, multiply cal/cm³ by 4.187). This table includes the polymer system

investigated, the method of evaluation, and when available, the evaluation temperature.^{11,12,32–39}

Three binary interaction energies are required to calculate the PPO/SAN interfacial thickness, namely: B_{PPO/S}, B_{S/AN}, and B_{PPO/AN}. The S/AN interaction has been estimated by various phase behavior observations, all of which report a value of about B_{S/AN} = 7.0 cal/cm³. Reports of B_{PPO/S} included in Table 2 span a range of -0.52 to -0.34 cal/cm³. A number of evaluation techniques including observations of phase behavior, small-angle neutron scattering (SANS), forward recoil spectrometry (FRES), and calorimetry have been used.^{12,34–37,40} Maconnachie et al.³⁴ investigated B_{PPO/S} as a function of temperature by SANS. A fit to their data gives: χ_{PPO/S} = 0.121 - 77.9/T, where χ is a Flory–Huggins-type interaction parameter. The latter is related to the binary interaction density, B, by

$$\chi = \frac{BV_{\text{ref}}}{RT} \quad (7)$$

where V_{ref} is a reference volume that usually is taken as the molar volume of some repeat unit. Because the molar volumes of PS and PPO repeat units are similar, an average value of V_{ref} = 106

cm³/mol is used here for conversion of the $\chi_{\text{PPO/S}}$ parameter to $B_{\text{PPO/S}}$.⁴⁰ A value of $\chi_{\text{PPO/S}} = -0.068$ is calculated at the 140°C annealing condition which, using eq. (7), corresponds to an estimate of $B_{\text{PPO/S}} = -0.52$ cal/cm³. Composto et al.³⁷ adjusted the temperature-dependent $\chi_{\text{PPO/S}}$ values reported by Maconnachie to $\chi_{\text{PPO/S}} = 0.145 - 78/T$ to allow for an improved fit to their FRES diffusion data. Using this modification, a value of $B_{\text{PPO/S}} = -0.34$ cal/cm³ is calculated at 140°C. Several estimates of the PPO/S interaction reported in the literature have been omitted from Table II. Those made by heat of dilution^{41,42} or melting point depression⁴³ measurements were left out because, in general, they tend to be several times larger (more favorable) than estimates made by more refined methods. Additionally, a significantly larger estimate determined from the phase behavior of PS and PPO brominated derivatives³³ was not included in Table II because it required the extraction of several unknown interaction parameters from only limited experimental data.

The work of Kressler and Kammer can be combined with eq. (5) and estimates for $B_{\text{PPO/S}}$ and $B_{\text{S/AN}}$ to arrive at an estimate for $B_{\text{PPO/AN}}$. They report the miscibility boundary of SAN copolymers with PPO to lie, depending on temperature, somewhere between 9.8 to 12.4 wt % AN; blends with less than 9.8 are miscible at all temperatures, those with more than 12.4 are immiscible at all temperatures, and those with compositions in between show lower critical solution temperature (LCST)-type phase separation. At the miscibility boundary, the overall B in eq. (5) is exactly balanced by the entropic contribution to mixing, such that $B = B_{\text{critical}}$ where

$$B_{\text{critical}} = \frac{RT}{2} \left(\sqrt{\frac{\rho_A}{(\bar{M}_w)_A}} + \sqrt{\frac{\rho_B}{(\bar{M}_w)_B}} \right)^2 \quad (8)$$

A value of $B_{\text{critical}} = 0.029$ cal/cm³ was calculated for this system using $M_w = 35,000$ for PPO and $M_w = 140,000$ for SAN. With the established estimate of $B_{\text{S/AN}} = 7.0$ and $B_{\text{PPO/S}} = -0.52$, $B_{\text{PPO/AN}}$ is estimated to lie between 10.7 and 12.0 cal/cm³. If $B_{\text{PPO/S}} = -0.34$ is used instead, the estimated $B_{\text{PPO/AN}}$ lies between 9.2 and 10.1 cal/cm³. A more refined estimate can be made based on the observation that a PPO blend with SAN containing approximately 11.5 wt % AN has a phase separation temperature of 140°C. From this, estimates of $B_{\text{PPO/AN}} = 11.3$ or $B_{\text{PPO/AN}} = 9.7$

are calculated, with $B_{\text{PPO/S}}$ set at -0.52 or -0.34 cal/cm³, respectively.

In addition to the value for $B_{\text{PPO/S}}$ discussed above, estimates for $B_{\text{S/MA}}$ and $B_{\text{PPO/MA}}$ are required to calculate the PPO/SMA interfacial thickness. Two independent reports based on phase behavior observations estimate a $B_{\text{S/MA}}$ of approximately 10.8 cal/cm³ at 140°C. Using the miscibility boundary of SMA copolymers with PPO, which lies between 10 and 12.2 wt % MA in the copolymer, $B_{\text{PPO/MA}}$ was estimated to have a value of 14.2 to 15.1 cal/cm³. This is even more unfavorable than the PPO/AN interaction. Here, $B_{\text{PPO/MA}}$ was recalculated using these same miscibility boundaries but with $B_{\text{S/MA}}$ set at 10.8 and with $B_{\text{PPO/S}}$ set at either -0.52 or -0.34 cal/cm³. The recalculated range is 13.4 to 16.6 cal/cm³, which is slightly wider than reported previously because of the allowance for uncertainty in $B_{\text{PPO/S}}$.

For this study, the temperature dependence of the binary interactions was approximated using an equation-of-state based correction that considers the compressible nature of the system. Characteristic parameters used in these calculations have been reported previously in the literature. In most cases, corrections of the binary interaction energies to the 140°C annealing condition are small. These values are reported in Table II. An annealing temperature of 180°C was also investigated in this study, but interactions corrected to this temperature vary only slightly from those calculated at 140°C.

Equation (5) was used with binary interaction energies that fall within the range of values reported in Table II to calculate $B_{\text{PPO/SAN}}$, while the analogue to eq. (5) for PPO/SMA was used to calculate $B_{\text{PPO/SMA}}$. The results, shown in Figure 2, predict an increase in the interaction energy as a function of copolymer composition with the dependence being notably stronger for the PPO/SMA interaction energy. These results are incorporated into interfacial thickness calculations presented later in this article.

PPO/SAN INTERFACE

The neutron reflectivity profiles from as-cast dPPO/SAN samples show regular, undamped interference patterns characteristic of well-defined interfaces. After annealing at 140°C for 1.5 h under vacuum, the neutron reflectivity profiles shown in Figure 3 were measured. In general, as the AN content in the SAN copolymer

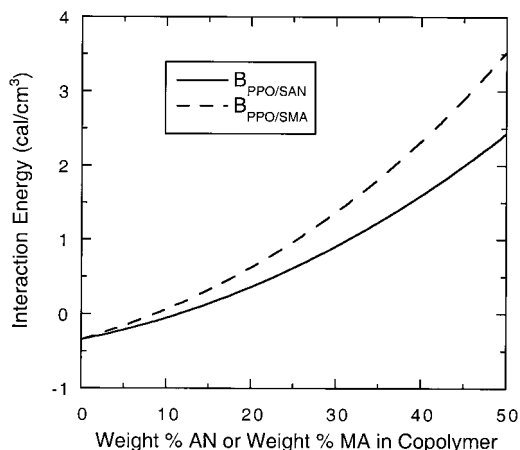


Figure 2. Calculated Flory–Huggins interaction energies at 140°C for PPO with SAN (solid line) and SMA (dashed line) as a function of copolymer composition. Curves are based on the following binary interaction parameters: $B_{\text{PPO/S}} = -0.34$, $B_{\text{S/AN}} = 7.0$, $B_{\text{PPO/AN}} = 9.2$, $B_{\text{S/MA}} = 10.8$, and $B_{\text{PPO/MA}} = 15.0 \text{ cal/cm}^3$.

decreases from 40 to 15 wt %, the interference pattern becomes more dampened, especially at larger wave vectors, indicating an increasingly

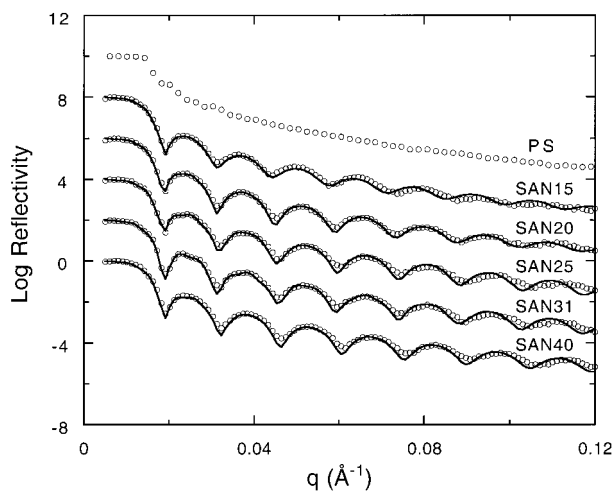


Figure 3. Composite plot of reflectivity profiles measured following annealing at 140°C for 1.5 h (offset from one another by two decades in $\log R$) for the interface between dPPO and PS, and between dPPO and various SAN copolymers. Open circles represent reflectivity data, while the solid curves represent the best-fit of a reflectivity model to the data. Interference oscillations are not detected in the miscible dPPO/PS sample (top curve). This interface is out of the resolution of NR measurements and, therefore, not fit. For increasing AN content in the copolymer the interface becomes increasingly sharp, as evidenced by the dampening of interference oscillations.

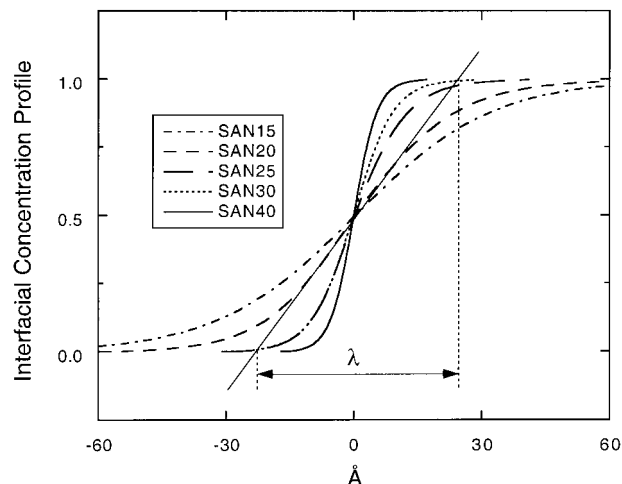


Figure 4. Interfacial profiles between dPPO and SAN copolymers extracted from model fits to the reflectivity profiles shown in Figure 3. The interpretation of λ , which corresponds to the definition of interfacial width in the Helfand–Tagami theory, is demonstrated.

diffuse interface. Further annealing of the dPPO/SAN bilayers at 140°C for 9 h and then at 180°C for 0.5 h produced little or no discernible change in the profiles. For comparison, the reflectivity profile from a bilayer sample of dPPO and PS, prepared and tested under similar conditions, is included in Figure 3. Distinct interference oscillations are absent from this reflectivity profile, owing to the miscibility of the two polymers.

For each sample, an estimate of the interfacial profile was made by fitting a reflectivity model to the NR data. The model accounts for the thickness and neutron scattering density of each polymer layer, for surface roughness, and for a diffuse interface between the polymer layers modeled as either an error function or hyperbolic tangent shaped profile. Because the Helfand–Tagami theory involves a hyperbolic tangent function, all fits to the neutron reflectivity data were made using a shape of this form. From a best model fit to each NR profile, shown as the solid line curves in Figure 3, the interfacial profiles presented in Figure 4 were estimated. A trend of decreasing interpenetration distance with increasing AN content in the copolymer is observed. By and large, the predicted interfaces are symmetric.

As illustrated in Figure 4, interfacial thickness was calculated graphically from the width of a tangent drawn to the inflection of the interfacial profile. This measurement corresponds to the interfacial thickness obtained from the analytical

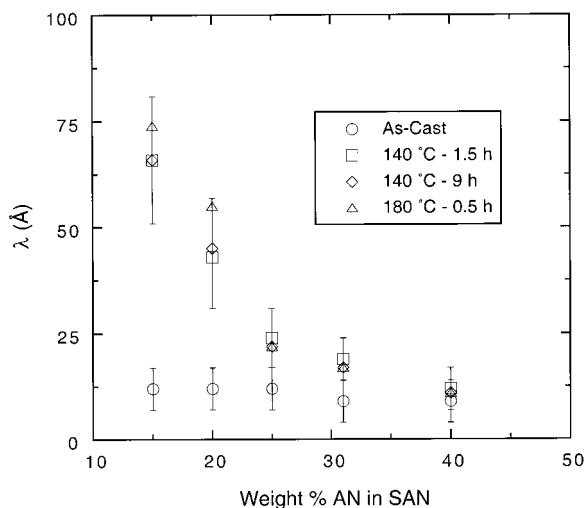


Figure 5. Interfacial thickness vs. copolymer composition measured by neutron reflectivity for dPPO/SAN samples as cast and following various annealing treatments. The as-cast samples have narrow interfacial widths reflecting reasonably good sample preparation.

expression for the theoretically assumed hyperbolic tangent profile. This method of evaluating λ is directly comparable with the Helfand–Tagami theory. Figure 5 is a plot of λ vs. SAN copolymer composition and includes measurements of the samples as cast and following each annealing treatment. Error bars denote the resolution limits of neutron reflectivity and for more diffuse interfaces indicate the loss of contrast. They were estimated by noting the range of λ over which the fit of the model to the data was acceptable; this corresponds to a chi-squared value of approximately 25 and smaller. The as-cast interfaces were estimated to be approximately 10-Å thick, independent of copolymer composition. This observation is important in that it indicates the consistency and quality of sample preparation. Following annealing of the samples for 1.5 h at 140°C, a trend developed with λ increasing from approximately 10 Å to 65 Å as the copolymer composition decreased from 40 to 15 wt % AN. As shown, these measurements were unaffected by an additional 9 h of annealing at 140°C and, therefore, are believed to closely approximate equilibrium values. Furthermore, these widths are representative of a narrow interface, and thus, comparison to the Helfand–Tagami theory should be valid. When these same samples were further annealed at 180°C for 0.5 h, a slight increase in λ was recorded in two of samples but the observations are within experimental error of the values measured at 140°C.

The neutron reflectivity measurements for dPPO/SAN interfaces are compared with predictions by the theory of Helfand and Tagami in Figures 6(a) and (b). For presentation purposes, only the data points corresponding to annealing condition of 140°C for 1.5 h are shown. The calculations account for molecular weight considerations using eq. (6) and use interaction energies summarized in Table II. The trend identified in Figure 2 of an increasingly unfavorable PPO/SAN interaction energy with increasing AN content is incorporated into the λ calculations according to eqs. (5) and (6). This contributes to asymptotic increase in interfacial width as the copolymer composition is lowered to the miscibility limit (i.e., neglecting molecular weight effects, as $B_{\text{PPO/SAN}}$ approaches a value of zero). The various predictions shown in the two figures explore the uncertainty in the value of the PPO/S interaction

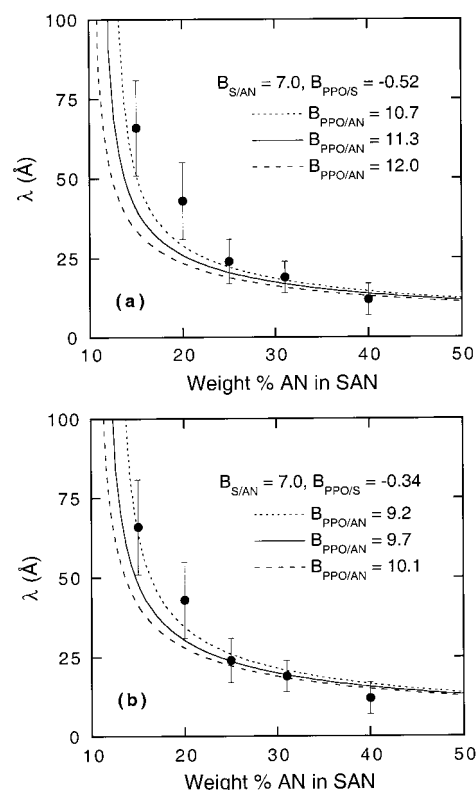


Figure 6. Comparison of dPPO/SAN interfacial thickness (samples annealed at 140°C for 1.5 h) with theoretical predictions using $B_{\text{S/AN}} = 7.0$, (a) $B_{\text{PPO/S}} = -0.52$, and (b) $B_{\text{PPO/S}} = -0.34$ cal/cm³, while varying $B_{\text{PPO/AN}}$ over a range of estimated values. The best fit of the data is found using the following set of binary interaction energies: $B_{\text{S/AN}} = 7.0$, $B_{\text{PPO/S}} = -0.34$, and $B_{\text{PPO/AN}} = 9.2$ cal/cm³.

which is coupled, as discussed in the preceding section on binary interactions, with the estimates used for the PPO/AN interaction energy. The three predicted curves in Figure 6(a) use $B_{S/AN} = 7.0$, $B_{PPO/S} = -0.52$ and $B_{PPO/AN}$ values ranging from 10.7 to 12.0 cal/cm³. This value of $B_{PPO/S}$ reflects the most favorable interaction reported in Table II. Alternatively, if a $B_{PPO/S}$ of -0.34 cal/cm³ is used, the least favorable interaction reported, with corresponding $B_{PPO/AN}$ values that fall within the range of 9.2 to 10.1 cal/cm³, the three curves shown in Figure 6(b) are predicted.

In both Figure 6(a) and (b), the general magnitude of the predicted interfacial thickness as well as the trend with changing copolymer composition is in reasonably good agreement with the neutron reflectivity measurements. Of these, perhaps the best correlation with measurements is shown as the narrow dashed-line curve in Figure 6(b), which is based on the following set of parameters: $B_{S/AN} = 7.0$, $B_{PPO/S} = -0.34$, and $B_{PPO/AN} = 9.2$ cal/cm³. As appropriate, this set of parameters may offer refinements to the range of values reported in Table II.

Even though the identified set of binary interactions accurately predicts the λ measurements, it must be recognized that there is some tolerance of the curve fit to slight variations in each parameter within this set. To quantify this, the sensitivity of the fit to each interaction was evaluated systematically by holding two of the interaction energies constant and varying the third while monitoring the agreement between the predicted and measured values of interfacial thickness. Only slight variations of ± 0.5 cal/cm³ for both $B_{PPO/AN}$ and $B_{S/AN}$, and of ± 0.05 cal/cm³ for $B_{PPO/S}$ were tolerated before the correlation became unacceptable. These tolerance levels are low, corresponding to less than 10% of the interaction values, and attest that only a well-defined set of binary interactions can produce good agreement between experiment and theory.

The agreement shown here between theory and experiment is significant. Problems arising from sample roughness seem to have been precluded by careful sample preparation as evidenced by the uniform and narrow as-cast interfaces. Perhaps more importantly, the interfaces studied here were all less than 100 Å thick. These should arguably qualify as strongly segregated and, thus, validate comparison with the Helfand–Tagami theory.

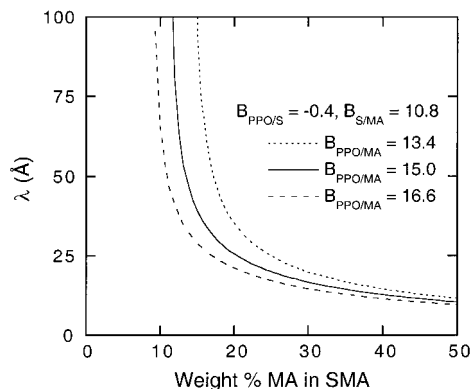


Figure 7. Prediction of the PPO/SMA interface using the Helfand–Tagami theory shows a stronger dependence on copolymer composition as compared to that for SAN in Figure 6.

PPO/SMA INTERFACE

Bilayers of dPPO/SMA were also studied by neutron reflectivity, but because of the sample preparation difficulties outlined in the Experimental section, these measurements were less reliable than those for the dPPO/SAN interfaces. Nonetheless, they provide order of magnitude estimates for comparison with theory, and identify trends with changing copolymer composition. The interface roughness of the as-cast samples measured approximately 30 to 50 Å thick, considerably broader and less uniform than the dPPO/SAN as-cast interfaces. After annealing the dPPO/SMA samples at 140°C for 3 to 8 h, the interference oscillations in the dPPO/SMA8 sample were effectively replaced by total film thickness oscillations, suggesting miscibility with dPPO. For the dPPO/SMA14 sample, the reflectivity profile was highly dampened at large wavevectors but distinct oscillations at smaller wavevectors indicated a broad (>200 Å), yet immiscible interface. The dPPO/SMA33 interference pattern was well defined, corresponding to an interfacial thickness of approximately 60 Å. These results are consistent with previous reports that located the miscibility boundary somewhere between blends containing 10 to 12.2 wt % MA in the SMA copolymer.

Figure 7 shows Helfand–Tagami predictions of the PPO/SMA interface. The calculations are based on physical parameters listed in Table I and estimates of $B_{S/MA} = 10.8$, $B_{PPO/S} = -0.4$, and values of $B_{PPO/MA}$ ranging from 13.4 to 16.6 cal/cm³. The value of $B_{PPO/S} = -0.4$ cal/cm³ was

chosen for demonstration purposes because it falls roughly in the center of the range of values summarized in Table II. Depending on the value of $B_{\text{PPO/SAN}}$ and $B_{\text{PPO/MA}}$ used in the calculations, however, the shape of the profile with respect to copolymer composition can shift considerably. Nonetheless, experimental observations suggesting the miscibility of SMA8 with PPO is consistent with all predictions. The blend with SMA14 falls within the range of the graph where the choice of binary interaction parameter values can significantly alter the shape of the prediction. An interfacial width larger than 200 Å is consistent with the predictions. Finally, the SMA33 blend is predicted to be immiscible but with an interface much smaller than the 60 Å that was measured. This disagreement is likely an artifact of sample preparation.

Compared to PPO/SAN interfaces, PPO/SMA interfaces are predicted to have a much stronger dependence on copolymer composition. To a large extent, this arises from the stronger dependence of $B_{\text{PPO/SMA}}$ on copolymer composition demonstrated in Figure 2. Although quantitative agreement between theory and experiments could not be confirmed, this study does verify the steep dependence of the dPPO/SMA interfacial width on MA content.

CONCLUSIONS

The interfacial thickness between immiscible blends of dPPO with SAN copolymers containing 15 to 40 wt % AN was measured by neutron reflectivity. Independently, the interfacial thickness was predicted using the theory of Helfand–Tagami coupled with a binary interaction model that utilizes experimentally determined estimates for binary interaction energies between repeat units. Both theory and experiment show an interface that broadens exponentially as the AN content in the copolymer decreases toward the miscibility limit. Depending on the choice of binary interaction energies selected from within the range of previously reported values, it was possible to find accurate quantitative agreement between experiment and theory. The interface between dPPO and SMA copolymers was also investigated and qualitative trends established that are in agreement with theory. The results of this study suggest that, at least for the PPO/SAN system, the Helfand theory adequately describes the

polymer–polymer interface and that the binary interaction model captures the nature of intermolecular and intramolecular interactions as quantified by binary interaction energies. Future work will expand this strategy to include other immiscible homopolymer/copolymer blends of commercial interest.

Financial support for this work has been provided by the National Science Foundation grant numbers DMR 92–15926 and DMR 97–26484 administered by the Division of Material Research—Polymers Program. The authors wish to thank Professor Peter F. Green for many insightful discussions on finite size effects.

REFERENCES AND NOTES

1. T. P. Russell, *Mater. Sci. Rep.*, **5**, 171 (1990).
2. N. Torikai, I. Noda, A. Karim, S. K. Satija, C. C. Han, Y. Matsushita, and T. Kawakatsu, *Macromolecules*, **30**, 2907 (1997).
3. T. L. Mansfield, Ph.D. Dissertation, University of Massachusetts (1993).
4. T. A. Callaghan, K. Takakuwa, and D. R. Paul, *Polymer*, **34**, 3796 (1993).
5. V. H. Watkins and S. Y. Hobbs, *Polymer*, **34**, 3955 (1993).
6. M. L. Fernandez and J. S. Higgins, *Polymer*, **29**, 1923 (1988).
7. The interfacial roughness of 20 Å reported by Fernandez et al. was shown by Anastasiadis et al. in ref. 8 to correspond to an interfacial thickness of 50 Å.
8. S. H. Anastasiadis, T. P. Russell, S. K. Satija, and C. F. Majkrzak, *J. Chem. Phys.*, **92**, 5677 (1990).
9. Anastasiadis et al. in ref. 8 found the PS/PMMA interfacial thickness to be 50 Å, independent of whether the interface was between a bilayer of the homopolymers or between the lamellar microdomains formed by diblock copolymers of PS and PMMA. Furthermore, the interfacial thickness was found to be independent of the molecular weight of the copolymer blocks.
10. T. A. Callaghan and D. R. Paul, *Macromolecules*, **26**, 2439 (1993).
11. C. K. Kim and D. R. Paul, *Polymer*, **33**, 2089 (1992).
12. P. P. Gan and D. R. Paul, *J. Appl. Polym. Sci.*, **54**, 317 (1994).
13. S. H. Anastasiadis, I. Gancarz, and J. T. Koberstein, *Macromolecules*, **21**, 2980 (1988).
14. P. C. Ellingson, D. A. Strand, A. Cohen, R. L. Sammler, and C. J. Carriere, *Macromolecules*, **27**, 1643 (1994).
15. D. W. Schubert and M. Stamm, *Europhys. Lett.*, **35**, 419 (1996).
16. M. Sferrazza, C. Xioa, R. A. L. Jones, D. G. Bucknall, J. Webster, and J. Penfold, *Phys. Rev. Lett.*, **78**, 3693 (1997).

17. S. Yukioka and T. Inoue, *Polymer*, **34**, 1256 (1993).
18. J. Kressler, N. Higashida, T. Inoue, W. Heckmann, and F. Seitz, *Macromolecules*, **26**, 2090 (1993).
19. N. Higashida, J. Kressler, S. Yukioka, and T. Inoue, *Macromolecules*, **25**, 5259 (1992).
20. E. Helfand and Y. Tagami, *J. Polym. Sci., Polym. Lett.*, **9**, 741 (1971).
21. E. Helfand and A. M. Sapse, *J. Chem. Phys.*, **62**, 1327 (1975).
22. D. Broseta, G. H. Fredrickson, E. Helfand, and L. Leibler, *Macromolecules*, **23**, 132 (1990).
23. G. T. Dee and B. B. Sauer, *Macromolecules*, **26**, 2771 (1993).
24. C. K. Kim and D. R. Paul, *Polymer*, **33**, 4941 (1992).
25. The reference to these materials does not imply their recommendation or endorsement by the National Institute of Standards and Technology.
26. J. M. Barrales-Rienda and D. C. Pepper, *J. Polym. Sci., B*, **4**, 939 (1966).
27. P. J. Akers, G. Allen, and M. J. Bethell, *Polymer*, **9**, 575 (1968).
28. Y. Shimura, I. Mita, and H. Kambe, *J. Polym. Sci.: Part B: Polym. Phys.*, **2**, 403 (1964).
29. Y. Shimura, *J. Polym. Sci. A-2*, **4**, 423 (1966).
30. G. Glockner, *Eur. Polym. J.*, **15**, 727 (1979).
31. R. Endo, T. Hinokuma, and M. Takeda, *J. Polym. Sci., A-2*, **6**, 665 (1969).
32. M. Nishimoto, H. Keskkula, and D. R. Paul, *Polymer*, **30**, 1279 (1989).
33. P. P. Gan, D. R. Paul, and A. R. Padwa, *Polymer*, **35**, 1487 (1994).
34. A. Macconnachie, R. P. Kambour, D. M. White, S. Rostami, and D. J. Walsh, *Macromolecules*, **17**, 2645 (1984).
35. G. ten Brinke, F. E. Karasz, and W. J. MacKnight, *Macromolecules*, **16**, 1827 (1983).
36. G. ten Brinke, E. Rubinstein, F. E. Karasz, W. J. MacKnight, and R. Vukovic, *J. Appl. Phys.*, **56**, 2440 (1984).
37. R. J. Composoto, J. W. Mayer, E. J. Kramer, and D. M. White, *Phys. Rev. Lett.*, **57**, 1312 (1986).
38. J. Kressler and H. W. Kammer, *Acta Polym.*, **38**, 600 (1987).
39. G. D. Merfeld and D. R. Paul, *Polymer*, **39**, 1999 (1998).
40. S. Ziaee and D. R. Paul, *J. Polym. Sci., Part B: Polym. Phys.*, **34**, 2641 (1996).
41. N. E. Weeks, F. E. Karasz, and W. J. MacKnight, *J. Appl. Phys.*, **48**, 4068 (1977).
42. F. E. Karasz and W. J. MacKnight, *Pure Appl. Chem.*, **52**, 409 (1980).
43. J. Plans, W. J. MacKnight, and F. E. Karasz, *Macromolecules*, **17**, 810 (1984).
44. R. P. Kambour, J. T. Bendler, and R. C. Bopp, *Macromolecules*, **16**, 753 (1983).